Environmental Science & Technology

pubs.acs.org/est

Article

Contrasting Reactive Organic Carbon Observations in the Southeast United States (SOAS) and Southern California (CalNex)

Colette L. Heald,* Joost de Gouw, Allen H. Goldstein, Alex B. Guenther, Patrick L. Hayes, Weiwei Hu, Gabriel Isaacman-VanWertz, Jose L. Jimenez, Frank N. Keutsch, Abigail R. Koss, Pawel K. Misztal, Bernhard Rappenglück, James M. Roberts, Philip S. Stevens, Rebecca A. Washenfelder, Carsten Warneke, and Cora J. Young

Cite This: *Environ. Sci. Technol.* 2020, 54, 14923−14935

Read Online

ACCESS | Metrics & More | Article Recommendations | Supporting Information

ABSTRACT: Despite the central role of reactive organic carbon (ROC) in the formation of secondary species that impact global air quality and climate, our assessment of ROC abundance and impacts is challenged by the diversity of species that contribute to it. We revisit measurements of ROC species made during two field campaigns in the United States: the 2013 SOAS campaign in forested Centreville, AL, and the 2010 CalNex campaign in urban Pasadena, CA. We find that average measured ROC concentrations are about twice as high in Pasadena (73.8 μgCsm^{-3}) than in Centreville (36.5 μgCsm^{-3}). However, the OH reactivity (OHR) measured at these sites is similar (20.1 and 19.3 s^{-1}). The shortfall in OHR when summing up measured contributions is 31%, at Pasadena and 14% at Centreville, suggesting that there may be a larger reservoir of unmeasured ROC at the former site. Estimated O_3 production and SOA potential (defined as concentration × yield) are both higher during CalNex than SOAS. This analysis suggests that the ROC in urban California is less reactive, but due to higher concentrations of oxides of nitrogen and hydroxyl radicals, is more efficient in terms of O_3 and SOA production, than in the forested southeastern U.S.

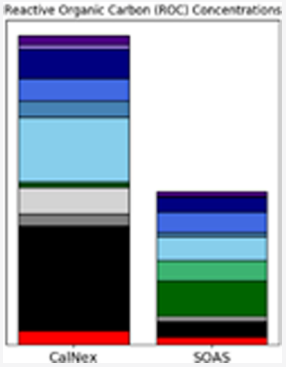

KEYWORDS: *atmosphere, reactive organic carbon, OH reactivity, SOA, ozone production*

1. INTRODUCTION

Reactive organic carbon (ROC, defined as the family of all atmosphere organics in any phase, other than methane[1]) compounds are emitted into the atmosphere from anthropogenic, pyrogenic, and natural sources,[2−4] whereupon they are oxidized primarily by OH, O_3, and NO_3 to form a suite of products, including particulate matter (PM), ozone, and CO_2.[5] At a global scale, models suggest that ROC is the dominant source for the production of these secondary species.[1,6,7] The first two of these secondary products, PM and O_3, are the principal global air pollutants, associated with the premature mortality of over 8 million people each year.[8] All three of these products impact climate, the last two as greenhouse gases, and organic aerosols that, through scattering and cloud formation, act to counterbalance some of the warming from greenhouse gases.[9]

Despite the central place of ROC in tropospheric chemistry, our understanding of its abundance, lifecycle, and ultimate impacts remain highly uncertain. This is largely due to the complexity of ROC, which is estimated to consist of many thousands of compounds,[10] a small subset of which are routinely measured and modeled in the atmosphere. Previous attempts to develop approaches to measure total carbon mass in the gas phase[11−13] have lacked the precision necessary to constrain a global budget. The alternative is to try to build a picture of the total mass of carbon by summing up speciated measurements from more routine instrumentation. Such an approach demonstrated that average observed ROC concentrations over North America spanned 2 orders of magnitude from 4 to 456 μgCm^{-3}.[14] This approach fails to identify whether carbon closure is achieved, but can provide insight into the abundance of key species of ROC and their fate. Over the last two decades, instrumentation has been developed to routinely detect a wider range of compounds.[5] The most comprehensive effort to date to sum measurements that span the range of volatility (and thus are thought to achieve mass closure), suggested that compounds that are not typically measured during field campaigns contributed ∼1/3 of the mass of ROC in a forested environment in Colorado.[15]

The atmospheric burden of ROC is dominated by long-lived species such as alkanes and acetone, whereas reactivity is dominated by short-lived species such as isoprene.[1] Together, these complementary metrics capture both those species

Received: July 28, 2020
Revised: November 12, 2020
Accepted: November 12, 2020
Published: November 18, 2020

Downloaded via MASSACHUSETTS INST OF TECHNOLOGY on July 5, 2021 at 18:34:51 (UTC).
See https://pubs.acs.org/sharingguidelines for options on how to legitimately share published articles.

ACS Publications © 2020 American Chemical Society

Table 1. Description of Measurements Used to Explore Reactive Organic Carbon during CalNex

measurement	instrument	operational dates during CalNex	uncertainty	reference	PI
OA	High Resolution Time of Flight Aerosol Mass Spectrometer (HR-ToF-AMS)	May 15 to June 16, 2010	38%	Hayes et al.,[24]	Jimenez
HCHO	Hantzsch reaction	May 15 to June 16, 2010	10%	Rappenglück et al.,[62]	Rappenglück
CHOCHO	Broadband Cavity Enhanced Absorption Spectrometer (IBBCEAS/CRDS)	May 15 to June 16, 2010	40 pptv + 15%	Washenfelder et al.,[38]	Washenfelder, Young
PAN, PPN	Gas Chromatograph with Electron Capture Detector (GC-ECD)	May 15 to June 16, 2010	15% + 0.005ppb, 20% + 0.005 ppb	Roberts et al.,[63]	Roberts
HNCO, HCOOH, acrylic acid, propionic acid, methacrylic acid, pyruvic acid	Negative Ion Proton Transfer Chemical Ionization Mass Spectrometer (NI-PT-CIMS)	May 15 to June 16, 2010	15−35%	Veres et al.,[64]	Veres and Roberts
Ethane, propane, *i*-butane, *n*-butane, *i*-pentane, *n*-pentane, hexane, nonane, undecane, ethene, propene, acetylene, 2-methyl-propene, 1-butene, *cis*2-butene, *trans*2-butene, 1,3-butadiene, benzene, toluene, *o*-xylene, *m*+*p*-xylene, 1-ethyl-benzene, styrene, ipropyl-benzene, npropyl-benzene, 1ethyl-3,4methyl-benzene, 1ethyl-2methy-benzene, 135TMB, 124TMB, 123TMB, 13dichlorobenzene, isoprene, α-pinene, β-pinene, limonene, acetaldehyde, propanal, butanal, benzaldehyde, acetone, MVK, methacrolein, 2-butanone, methanol, ethanol, iso-propanol, bromoform, DMS, acetonitrile, 2,3-butadione	Gas Chromatography Mass Spectrometer (GC-MS-TACOH)	May 15 to June 16, 2010	15−25% for hydrocarbons, 20−35% for oxygenates	Kuster et al.,[65]	Gilman
2methyl-pentane, 3methyl-pentane, *n*-heptane, 2methyl-hexane, 3methyl-hexane, i-octane, *n*-octane, methyl-acetate, 1,3-methyl-butene, trichlorofluoromethane, trichloroethene, chloroform, dichloromethane, cyclohexane, *cis*1,3dimethyl-cyclohexane, methyl-cyclohexane, *trans*1,2dimethyl-cyclohexane, trans1,3dimethyl-cyclohexane, methyl-cyclopentane, methyl-formate, 3-furanaldehyde, *n*-hexanal, nitromethane, 2methyl-propanal, 2-propenal, vinyl-acetylene, ethyl-nitrate	extended analysis of GC-MS	May 15 to June 16, 2010		McDonald et al.,[22]	Gilman
total monoterpenes	Proton Transfer Reaction Ion Trap Mass Spectrometer (PIT-MS)	May 15 to June 16, 2010	15−25%	Warneke et al.,[66]	Warneke, de Gouw, Graus
OH, HO_2, OHR	Fluorescent Assay by Gas Expansion	May 15 to June 16, 2010	38% (OH, HO_2), 30% (OHR)	Griffith et al.,[41] Hansen et al.[67]	Stevens
O_3, SO_2, NO, NO_2	Thermo Scientific (49c, 48i-TLE, 42i-TL)	May 16 to June 16, 2010	4%, 4%, 4%, 6%	Lefer et al.,[68] Luke et al.,[69] Pollack et al.[70] Drummond et al.[71]	Lefer
CO	VUV resonance fluorescence AeroLaser AL5002	May 15 to June 16, 2010	4%	Gerbig et al.,[72]	Holloway

https://dx.doi.org/10.1021/acs.est.0c05027
Environ. Sci. Technol. 2020, 54, 14923−14935

Table 2. Description of Measurements Used to Explore Reactive Organic Carbon during SOAS

measurement	instrument	operational dates during SOAS	uncertainty accuracy	reference	PI
organic aerosol	High Resolution Time of Flight Aerosol Mass Spectrometer (HR-ToF-AMS)	June 6 to July 15, 2013	38%	Hu et al.,[73]	Jimenez
HCHO	Fiber-Laser-Induced Fluorescence (FiLIF-II)	June 1 to July 15, 2013	15%	DiGangi et al.,[74] Hottle et al.[75]	Keutsch
CHOCHO	Madison Laser-Induced Phosphorescence (Mad-LIP)	June 1 to July 15, 2013	9%	Huisman et al.,[76]	Keutsch
Formic acid, HCN, HAC (hydroxyacetone), PAA (peroxyacetic acid), $C_5H_8O_3$ (HPALD), $C_5H_{10}O_3$ (IEPOX+ISOPOOH), ethanol nitrate, propanone nitrate, isoprene nitrate	Caltech Chemical Ionization Time of Flight Mass Spectrometer (CIT-ToF-CIMS)	June 1 to July 3, 2013	100 ppt + 30−50% [X]	Nguyen et al.[77]	Wennberg
PNs (peroxynitrates)	Thermal Dissociation-Laser-Induced Fluorescence (TD-LIF)	June 1 to July 15, 2013	15%	Romer et al.,[78]	Cohen
Ethane, ethene, propane, propene, ethyne, *i*-butane, *n*-butane, i-pentane, *n*-pentane, *n*-hexane, *n*-decane, benzene, toluene, 1ethyl-benzene, *m*-xylene+*p*-xylene, *o*-xylene, 1ethyl-3and4methyl-benzene, 135TMB, 124TMB, isoprene, α-pinene, β-pinene, limonene, camphene, myrcene, *p*-cymene, acetaldehyde, methanol, ethanol, propanal, butanal, benzaldehyde, acetone, MVK, methacrolein, MEK, DMS, acetonitrile, butadiene-23, 1ethyl-nitrate, ipropyl-nitrate	Gas Chromatography Mass Spectrometer (GC-MS TACOH)	June 1 to July 15, 2013	20%	Gilman et al.,[79]	Goldstein & de Gouw
total monoterpenes	Proton Transfer Mass Spectrometer (PTR-MS)	June 16 to July 5, 2013	20%	Graus et al.,[80]	Goldstein, Guenther
3-hydroxyglutaric acid, pinic acid, pinonic acid, 2-methylthreitol, 2-methylerythritol, 3methyl-2,3,4-trihydroxy-butene, *cis*2methyl-1,3,4, trihidroxy-butene, 2-methylglyceric acid, levoglucosan	Semi-Volatile Thermal desorption Aerosol Gas chromatograph (SV-TAG)	June 4 to July 15, 2013	20%	Isaacman Van Wertz et al.,[30]	Goldstein
OH, HO_2, OHR	Ground Based Tropospheric Hydrogen Oxides Sensor (GTHOS)	June 1 to July 15, 2013	2%, 20%	Feiner et al.,[40] Faloona et al.[81]	Brune
O_3	Thermo Scientific UV absorption (49i)	June 1 to July 15, 2013	6.1%		operated by SEARCH network
CO	Thermo Scientific, IR absorption with gas filter correlation (GFC) (48i)	June 1 to July 15, 2013	7.4%		operated by SEARCH network
SO_2	Thermo Scientific, pulsed UV fluorescence (43i)	June 1 to July 15, 2013	6.1%		operated by SEARCH network
NO, NO_2	Thermo Scientific, Chemiluminscence (42i)	June 1 to July 15, 2013	5.5%, 15%		operated by SEARCH network

https://dx.doi.org/10.1021/acs.est.0c05027
Environ. Sci. Technol. 2020, 54, 14923−14935

highest in abundance and those most important for chemical processing. Techniques to measure total OH reactivity (OHR, the inverse of the OH lifetime) were developed over a decade ago, and are now routinely deployed in field campaigns (see Yang et al.[16] for a review). OHR is typically dominated by ROC, other than in some urban or remote environments where the bulk of OHR may come from inorganics or long-lived species (e.g., CH_4, CO), respectively.[17−19] When deployed alongside speciated measurements, OHR measurements can be used to estimate the "missing OHR" not accounted for by routine instrumentation. This missing OHR has been estimated at 30−50% in urban environments, and higher (more than half missing in some cases) in forests.[16] This missing OHR may represent unmeasured emitted species or oxidation products.

While the measurements of OHR provide a powerful framework to assess chemical processing in the atmosphere, it is crucial to acknowledge that the term "missing reactivity" has been applied somewhat fluidly. The "missing reactivity" can be the shortfall between the contribution from measured species and the total OHR measurement (as described above and used in this study), or it can be the difference between modeled OHR and the total OHR measurement. The former having the virtue of a direct constraint, the latter accounting for known unmeasured compounds. When "missing reactivity" is assessed based solely on measurements, it reflects the suite of instrumentation deployed under varying operating conditions in any given campaign (which may, for example, dictate detection limits and the number of species reported). This suite can be more or less comprehensive, and is certainly not consistent across campaigns, challenging our ability to compare "missing reactivity" estimates. The summed reactivity also relies on assumed rate constants, which may differ across studies. Furthermore, the measurement of total OHR is itself operationally defined. For example, some semivolatile or intermediate volatility compounds (S/IVOC) may not be sampled through an inlet, or chemical reactions may rapidly reform OH, resulting in the measured OH loss being lower than the OHR calculations that do not consider this recycling. These definitional and operational factors may influence the interpretation of OHR results.

Field observations provide a snapshot of the local atmospheric environment and can be used to probe specific sources and atmospheric processes. While field campaigns are often constructed with specific scientific questions in mind, the observational capital may be relevant to additional future lines of inquiry. In this study, we revisit measurements made during two field campaigns over the United States: the Southern Aerosol and Oxidant Study (SOAS) of 2013 and the California Research at the Nexus of Air Quality and Climate (CalNex) campaign of 2010. While numerous studies have explored the processes controlling atmospheric composition for each of these two campaigns, this study applies a new lens to contrast the abundance and role of ROC in these two very different environments.

2. MATERIALS AND METHODS

The CalNex campaign was based in Southern California, a region which has undergone a major air quality cleanup since the 1970s but remains under the influence of over 10 million people who live in Los Angeles County.[20] Southern California represents a modern urban environment, characterized by reductions in vehicle emissions over recent decades,[21] with increasingly important emissions from other source categories including volatile consumer products (VCPs).[22] Here we investigate measurements made at the Pasadena, California ground site from May 15 to June 16, 2010, from towers located 10 m above an empty parking lot (note that the AMS had a separate inlet sampling above a trailer at a height of ∼6m). See Table 1 for details and Ryerson et al.[20] for more information. In particular, we include here an expanded set of ROC measurements made by gas chromatography mass spectrometry (GC-MS) based on new peak identification methods.[22,23] A 2D-TAG was deployed during the last 4 days of the campaign, but given the lack of overlap with other measurements, that data is not included here.[24,25] Meteorological conditions varied during the CalNex campaign with both sunny, clear days and cool, overcast days.[20]

SOAS was a part of the larger Southeast Atmospheric Study (SAS) of 2013.[26] The Southeast United States (SEUS) represents a mix of biogenic and anthropogenic sources, with urban centers embedded in large swaths of forests. Air quality regulations have led to declines in anthropogenic emissions of NO_x, SO_x, and organic aerosol in the region for more than a decade preceding SOAS.[27,28] Here we explore the measurements made at the ground site in Centreville, Alabama, from June 1 to July 15, 2013. The majority of the gas phase measurements analyzed here were made from a tower located 16.5 m above the ground in a clearing near the edge of a forest and well above the forest canopy (Table 2). The aerosol measurements and the gas phase measurements operated by the SEARCH network (see Table 2) were made nearby at ground-level near the center of the clearing. This rural site is located within the Talladega National Forest, a dense mixed forest of pine and broadleaf trees. The summer of 2013 was consistently cooler and rainier than average conditions.[26]

In this study, we revisit the online measurements of ROC, OH reactivity, and related trace species measured at Centreville and Pasadena. For both campaigns, all observations are first averaged to an hourly time base and individual ROC species concentrations are converted into units of μgCm^{-3} at standard temperature and pressure (STP, 298 K, 1 atm). Given that not all instrumentation operated continuously over the entirety of the campaigns, in particular for SOAS (see Table 2), we only present diurnal averages or 24-h averages for each campaign. We further note that while much of the same key instrumentation was deployed at both sites, this suite and its operation are not identical, and not all species are observed at concentrations above detection limits at both sites, thus the list of ROC species measured/reported for the SOAS and CalNex campaigns differ.

3. RESULTS

3.1. Reactive Organic Carbon Mass Concentrations.

Figure 1 shows the average ROC mass concentrations measured for the CalNex and SOAS campaigns, highlighting the contributions from different chemical families. Table S1 of the Supporting Information (SI) provides average concentrations for each individual species.

Average ROC concentrations during SOAS total 36.5 $\mu gCsm^{-3}$, with sizable contributions from primary biogenic species, in particular isoprene (8.6 $\mu gCsm^{-3}$) and monoterpenes (4.8 $\mu gCsm^{-3}$). The top 10 species (isoprene, methanol, acetone, organic aerosol, ethanol, α-pinene, MVK, ethane, other monoterpenes, and β-pinene) contribute 70% of the mean ROC mass concentrations observed during SOAS. In

https://dx.doi.org/10.1021/acs.est.0c05027
Environ. Sci. Technol. 2020, 54, 14923−14935

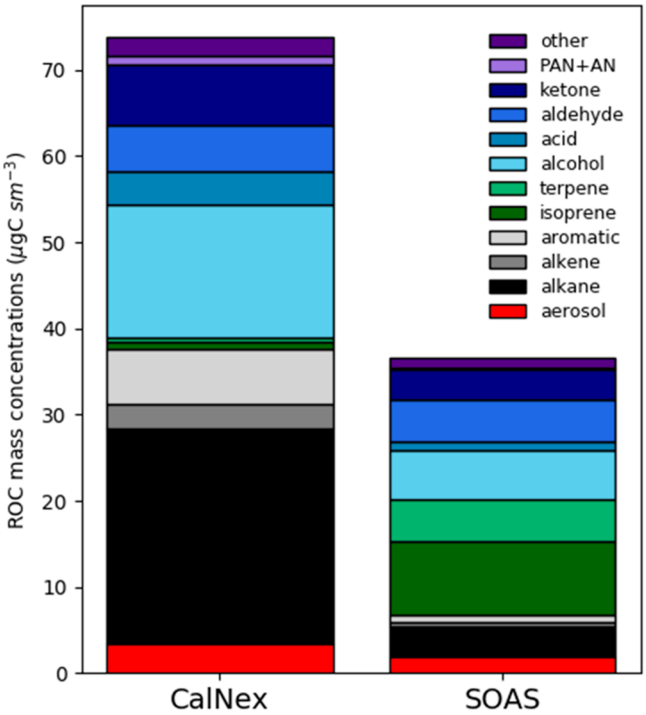

Figure 1. Average ROC mass concentrations for CalNex and SOAS field campaigns at standard temperature and pressure (STP).

contrast, CalNex ROC (average 73.8 μgCsm^{-3}) is dominated by anthropogenic species, including alkanes (24.9 μgCsm^{-3}) and ethanol (9.0 μgCsm^{-3}), the latter of which has been highlighted as a product of VCP emissions as well as from mobile sources in the Los Angeles region.[22,29] The top 10 species measured during CalNex (ethanol, acetone, ethane, propane, *i*-pentane, methanol, organic aerosol, propanol, propionic acid, and *n*-butane) make up 58% of the mean ROC. Overall, measured ROC is twice as abundant in the atmosphere during CalNex compared to SOAS, consistent with expectations of higher ROC in a "polluted environment". When compared to a previous compilation of ROC concentrations over North America,[14] the ROC reported at CalNex is second only to Mexico City, and exceeds ROC reported in Pittsburgh in 2002. Similarly, ROC levels during SOAS are higher than all nonurban sites reported in Heald et al.,[14] as well as the Manitou Forest site where Hunter et al.[15] report average ROC concentrations of 26.7 μgCm^{-3}. Despite the substantial differences in ROC abundance and speciation during CalNex and SOAS, we find that organic aerosol contributes ∼5% of ROC in both environments.

Figure 2a demonstrates that ROC concentrations peak in the early afternoon for both SOAS and CalNex. This maximum is driven by isoprene for SOAS (this daytime peak is dampened by the night-time peak in monoterpenes), and OA, acetone, and propane for CalNex. There are modest differences between weekday and weekend ROC, with slightly higher values (<10%) on weekends in both Pasadena and Centreville. The slightly higher weekend concentrations of biogenics such as isoprene during SOAS may be the result of lower NO_x and lower OH over the weekend extending the lifetime of these primary species.

We note that our analysis includes only the identified and calibrated S/IVOC (semivolatile to intermediate volatility, with saturation vapor pressures $C^* = 1-10^5$ μg m^{-3}) species

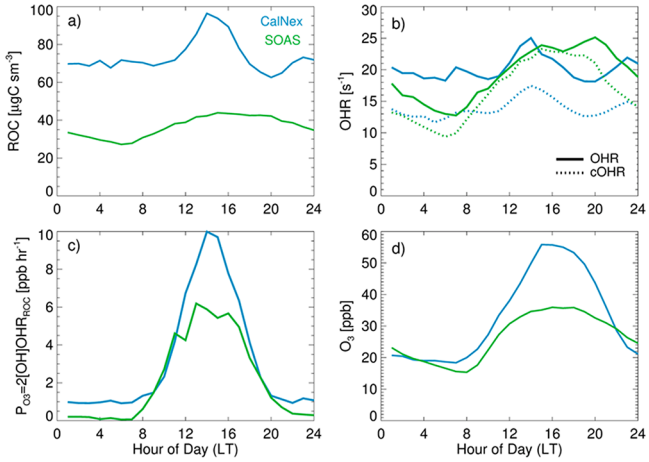

Figure 2. Mean diurnal cycle for CalNex (blue) and SOAS (green) campaigns of (a) observed ROC mass concentrations at STP, (b) observed OH reactivity and calculated OHR (cOHR, dotted lines), (c) estimated ozone production rate, and (d) observed O_3 mixing ratios.

measured by SV-TAG during SOAS;[30] these compounds contribute 0.25 μgCsm^{-3}. A preliminary calibration of all the additional SV-TAG measured compounds with the formulas $C_{15}H_{24}$ and $C_{15}H_{22}$,[31] which should provide an upper-bound on sesquiterpene concentrations, indicates that sesquiterpenes contribute less than 100 ngCm^{-3} throughout the SOAS campaign. It is not clear how much additional mass may be contributed by unmeasured/unidentified S/IVOC species. We also note that a nitrate CIMS was deployed during SOAS which detected an additional 87 compounds which make a negligible contribution to ROC mass concentrations (0.03 μgCsm^{-3}) and are not included in further analysis. No online speciated S/IVOC measurements are available during CalNex. Unspeciated gas-phase SVOC concentrations ($C^* = 1$ μg m^{-3}) estimated by Ma et al.[32] average 2.77 μg m^{-3} (assuming an OM:OC = 1.3, equivalent to ∼2.1 μgC m^{-3}), or less than 3% of the measured ROC. Zhao et al.[33] report 3-h integrated IVOC measurements (both speciated and unspeciated, equivalent to $C_{12}-C_{22}$ *n*-alkanes) made offline from Tenax glass tubes during CalNex, with a campaign average concentration of primary IVOC of 6.3 μgm^{-3} (assuming an OM:OC of 1.1 for a C15 *n*-alkane this gives ∼5.7 μgCsm^{-3}). This represents an additional 8% in ROC mass concentrations. Measurement and quantification challenges for these samples are discussed in Zhao et al.[33]

3.2. OH Reactivity. We translate the observed mass concentrations during CalNex and SOAS into calculated OH reactivity (cOHR), which is defined here as $\Sigma(k_{OH+Xi}[X_i])$, the sum of OH reactivity contributed by each species (X_i). We note that this includes not only ROC species, but also other key gas phase species that react with OH (CO, O_3, NO, NO_2, SO_2, OH, HO_2). We use here reaction rate constants (k_{OH+Xi}) at 298 K, taken from JPL kinetics compilation,[34] the IUPAC evaluated kinetic data[35] the GEOS-Chem chemical mechanism v12.7.0 (www.geos-chem.org), or from EPI Suite[36] (see Tables S1 and S2). As in Hunter et al.,[15] we make no effort to adjust reaction rates for ambient temperatures during SOAS and CalNex; this is reasonable for SOAS where average temperatures are similar to 298 K, but likely leads to a slight overestimate of cOHR at night during CalNex when temperatures drop to ∼288 K. Aerosols are not expected to

https://dx.doi.org/10.1021/acs.est.0c05027
Environ. Sci. Technol. 2020, 54, 14923−14935

contribute significantly to OHR. For example, following eq 3.[38] of Seinfeld and Pandis,[37] we calculate that under moderately polluted conditions (50 μgm^{-3}, assuming a mean diameter of 200 nm) the upper-limit first order rate coefficient for OH loss to particles (given an average molecular velocity of OH of 609 ms^{-1} and assuming an upper limit for the uptake coefficient of 1) is 0.23 s^{-1}, equivalent to ∼1% of the measured OHR during CalNex and SOAS (see below). It is therefore reasonable to neglect the aerosol contribution to OHR during these campaigns.

Figure 3 shows the average cOHR for CalNex and SOAS. The total cOHR for SOAS is 16.6 s^{-1}, with a large contribution of 9.4 s^{-1} from a single species, isoprene, and a further 0.7 s^{-1} from its immediate oxidation products MVK and methacrolein. Monoterpenes contribute an additional 2.9 s^{-1}. Over 85% of cOHR at the SOAS site is from ROC species, largely biogenics. By contrast, the average cOHR during CalNex (13.9 s^{-1}) is dominated by NO_x (4.7 s^{-1}), with ROC species contributing 51% of the reactivity. Despite the urban nature of this site, isoprene remains the single largest ROC contributor to reactivity during CalNex (0.9 s^{-1}), although the amount is an order of magnitude lower than that for SOAS. Washenfelder et al.[38] noted that oak and eucalyptus trees upwind of Pasadena likely represent a local biogenic source during CalNex. The second most important individual ROC contributor to reactivity during CalNex is acetaldehyde, a product of ethanol and alkene oxidation, concentrations of which have increased in ambient air, including over California, in recent decades due to ethanol fuel additives and VCP emissions.[22,29] In general, we find that many of the measured ROC species that contribute to mass concentrations during CalNex (Figure 1) do not substantially impact calculated reactivity (Figure 3), suggesting that OH loss in southern California is not primarily driven by anthropogenic (or biogenic) ROC emissions. The reactivity per mass concentration of ROC is more than 4 times higher for SOAS than for CalNex (0.10 for CalNex vs 0.42 for SOAS). However, we note that despite all of these differences, the total cOHR estimated for CalNex and SOAS are quite similar.

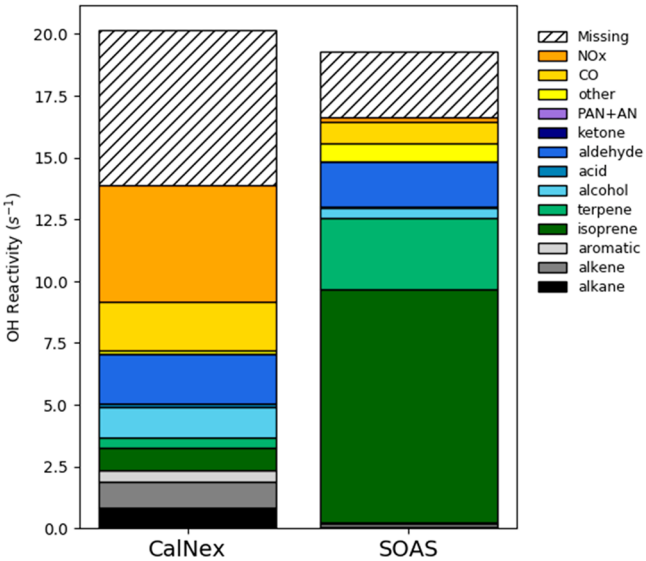

Figure 3. Average calculated OH reactivity for CalNex and SOAS field campaigns. The missing reactivity is defined as the difference between the measured total OH reactivity and the summed calculated OH reactivity. The uncertainty on individual OHR measurements is given as 30% and 20% for CalNex and SOAS, respectively (see Tables 1 and 2). The calculated standard error (defined as $\theta/\sqrt{N}$) on campaign average OHR is 0.32 s^{-1} and 0.28 s^{-1}, respectively (too small to be shown on the plot).

Figure 2b shows that the diurnal cycle for cOHR is even more muted during CalNex than ROC concentrations shown in Figure 2a, given that cOHR from highly reactive alkenes peaks at night,[39] compensating for the daytime peak driven by isoprene and acetaldehyde. The large contribution of isoprene to reactivity during SOAS enhances the diurnal cycle observed in ROC concentrations at that site (Figure 2a,b). Weekday and weekend differences in cOHR are negligible (not shown).

During both SOAS and CalNex, measurements of total OHR were deployed using laser-induced fluorescence techniques and both data sets were corrected for chemical interferences.[40,41] Thus, these measurements and the cOHR compiled here provide a critical opportunity to contrast the "missing OH reactivity" at two very different sites in the United States. However, as discussed in section 1, operational differences in measured OHR may remain. Measured OHR is similar at Pasadena and Centreville, with average values of 20.1 and 19.3 s^{-1}, respectively. Figure 3 shows that 31% and 14% of the measured reactivity is not accounted for by the cOHR (6.3 s^{-1} for for CalNex and 2.6 s^{-1} for SOAS). The "missing reactivity" for SOAS is well within the uncertainty of the OHR measurement and rate constants used to estimate cOHR, and may indicate that all the reactivity is accounted for at this site. Kaiser et al.[42] suggest that in their analysis missing OHR during SOAS may be attributed to unmeasured primary emissions (e.g., sesquiterpenes). Some studies[43,44] (though not all[45]) have shown that sesquiterpene concentrations peak at night, which may offer an explanation for Figure 2b showing a nighttime peak in missing OHR, with little missing OHR in the daytime. However, while sesquiterpene measurements made by SV-TAG during SOAS (see section 3.2) show a pronounced nighttime peak, concentrations were substantially lower than monoterpene concentrations, consistent with previous studies that suggest that sesquiterpene concentrations are relatively low outside of the forest canopy,[44] and thus unlikely to fully explain the missing OHR at night. In Pasadena, however, there may be a larger reservoir of unmeasured ROC species (or inorganics). As shown in McDonald et al.,[22] the ROC measurements during CalNex (including the expanded suite of species measured by GC-MS, see Table 1) capture much of the reactivity from VCP sources, however they also suggest that unmeasured ROC species from VCP sources could contribute additional OHR (see Table S8 of that study). An analysis of comprehensive ROC measurements at Manitou Forest in Colorado during 2011 suggested that previously unmeasured S/IVOCs compounds, contributed ∼25% of the OHR at that site. S/IVOC compounds may also make an important contribution to OHR in Southern California and in the SEUS. However, the subset of SVOCs measured by SV-TAG during SOAS contribute only 3% (0.56 s^{-1}) of the cOHR. Applying OH reaction rates to the average primary IVOCs concentrations measured offline during CalNex (see Tables S5 and S7 of ref 33), yields an additional 0.33 s^{-1} of cOHR, suggesting that these IVOC contribute only ∼5% of the missing OHR during CalNex. The missing OHR during CalNex appears to be consistent throughout the day (Figure 2b), and therefore is not suggestive of a clear local primary emission signature.

https://dx.doi.org/10.1021/acs.est.0c05027
Environ. Sci. Technol. 2020, 54, 14923−14935

3.3. Ozone Production. We can use the estimated cOHR to explore ozone formation associated with ROC during CalNex and SOAS. Ozone formation is initiated by the reaction of peroxy radicals with NO, as described by Jacob[46] and applied in Sinha et al.:[47]

$$P_{O3} = 2k[RO_2][NO] \quad (1)$$

with the resulting NO_2 photolyzing to produce ozone. If we assume the rapid cycling of radicals in a polluted atmosphere:

$$k_{OH+ROC}[ROC][OH] = k[RO_2][NO] \quad (2)$$

then,

$$P_{O3} = 2OHR_{ROC}[OH] \quad (3)$$

Figure 2c shows the estimated diurnal pattern in P_{O3} based on eq 3 for both CalNex and SOAS. As described in Section 3.2, CalNex is characterized by much lower ROC reactivity (7.1 s^{-1}) than SOAS (15.5 s^{-1}), however OH concentrations during CalNex are about a factor of 4 higher than during SOAS, with mid-day peaks of 4×10^6 and 1×10^6 molecules cm^{-3}, respectively. Thus, the resulting ozone production rate is about 50% higher during CalNex, with peak early afternoon values of ∼9 ppb hr^{-1}, compared to ∼6 ppb hr^{-1} for SOAS. We note that there is little weekday−weekend difference in measured OH during CalNex in contrast with estimated OH concentrations based on simple-steady state models;[48] constraining these estimates to measured OHR yields better agreement with measured OH.[41]

Figure 2d shows the mid-day increase in ozone concentrations observed during CalNex and SOAS. CalNex is characterized by ∼40 ppb increase over 7 h, with a more modest increase of ∼15 ppb over the same time interval for SOAS. These daytime increases likely reflect local production integrated over the immediate upwind region, as well as the mixing down of the residual layer from the previous day. The diurnal profile of typical ozone deposition velocities for urban and forested land classes[49] produce a small sink of 0.3−0.6 ppb hr^{-1} peaking mid-day; this is negligible compared to the daytime ozone production rates calculated at Pasadena and Centreville. The observed ozone increase in Southern California is roughly consistent with the ozone production rate calculated using eq 3, however this relationship appears to substantially overestimate the observed daytime increase in ozone in the SEUS. This is true even when the calculated ozone production rate is tempered by the estimated ozone dry deposition flux over forested land.

The lower ozone formation during SOAS is the result of NO_x limitations at this forested site. This can be illustrated by a metric ($\vartheta = OHR_{NOx}/OHR_{ROC}$) suggested by Kirchner et al.[50] to assess ozone production regimes. The observations at CalNex produce an average ϑ of 0.52 which is well above the 0.2 boundary to indicate VOC-limitation. Average early afternoon ϑ is lower on weekends due to lower NO, but stays above 0.35 consistent with VOC-limitation, whereas using an alternate metric Griffith et al.[41] suggest that observations during afternoons on weekends are NO_x-limited during CalNex. We note that if we assume that all of the missing OHR comes from unmeasured ROC species, the recalculated ϑ briefly dips below the 0.2 boundary on weekend afternoons suggesting a transition from VOC to NO_x limited. Conversely, the average ϑ at SOAS exhibits a strong diurnal cycle where ϑ drops below the NO_x limitation boundary (0.01) from 9am to 4 pm on average (on both weekday and weekends), and increases overnight (campaign average ϑ of 0.012). Thus, despite very high reactivity from ROC in the SEUS, the lower daytime OH and NO_x depress the ozone production potential of these organics during SOAS.

We note that the OHR from IVOC during CalNex discussed in Section 3.2 could contribute an additional ∼5% to the ozone production rate calculated using eq 3; well within the uncertainty associated with estimating the ozone production rate from its observed daytime increase in Figure 2c. However, if the remaining missing OHR during CalNex were attributed to ROC, then the resulting calculated ozone production would substantially exceed the observed rise in ozone concentrations. This suggests that either (1) some of the missing OHR may be the result of non-ROC species, or (2) conditions during CalNex may not be uniformly NO_x-saturated (as assumed in eq 3), reducing ozone production efficiency, or (3) that there are larger, unaccounted for, sinks of ozone during CalNex. Deployment of instrumentation at an upwind site, as well as an O_3 reactivity instrument,[51] alongside the suite of instrumentation deployed in Pasadena during CalNex, could provide further insight into the role of ROC in controlling ozone concentrations in the LA basin.

3.4. SOA Formation Potential. ROC oxidation leads to the formation of secondary organic aerosol (SOA), a substantial and sometimes dominant contributor to fine particulate matter.[52] The vast potential number of precursors which produce SOA at varying time scales, coupled with gaps in our understanding of this chemistry, combined with the addition of primary organic aerosol, complicate any assessment of regional SOA formation. Here we explore the instantaneous SOA formation potential of ROC at Centreville and Pasadena.

To estimate the SOA formation potential (the potential amount of SOA formed from the measured precursors), we multiply mass concentrations of ROC with carbon yields (Y_C) based on the approach of Hunter et al.[15] A subset of yields for more well-studied SOA precursors (aromatics, isoprene, and monoterpenes) are taken from Hunter et al.[15] based on chamber studies. The remaining yields are estimated based on the vapor pressure of each species taken from EPI Suite,[36] converted to the saturation vapor pressure (C^*), and then to yield using the functional form of Donahue et al.[53] (as given in caption of Table S1). The resulting yields vary from <1% to 19% (see Table S1). We employ this approach as it allows us to systematically estimate the SOA yields for all considered species, however, we note that the uncertainty on these estimated yields is high; Hunter et al.[15] suggest a factor of 3. While a detailed review of all estimated yields is beyond the scope of this study, we note that the systematic application of the relationship between vapor pressure and carbon yield[53] leads to large estimated yields for alcohols (Y_C = 3−5%), however, there is no laboratory evidence to date to suggest that the oxidation of alcohols yields appreciable SOA, in fact some previous CalNex studies assume that the SOA yield from alcohols is zero.[22,54] Thus, in what follows, we assume zero SOA potential for alcohols (SOA potentials for these species as calculated using the approach of Donahue et al.[53] are given in brackets in Table S1). In addition, we note that the SOA potential metric as used here only captures SOA formed in the gas-phase.

Figure 4 summarizes the SOA formation potential at Pasadena and Centreville. CalNex SOA formation potential is 1.46 $\mu gCsm^{-3}$, with large contribution from aromatics (0.45 $\mu gCsm^{-3}$, Y_C = 2−11%); propionic acid, toluene, and *m-p-*

https://dx.doi.org/10.1021/acs.est.0c05027
Environ. Sci. Technol. 2020, 54, 14923−14935

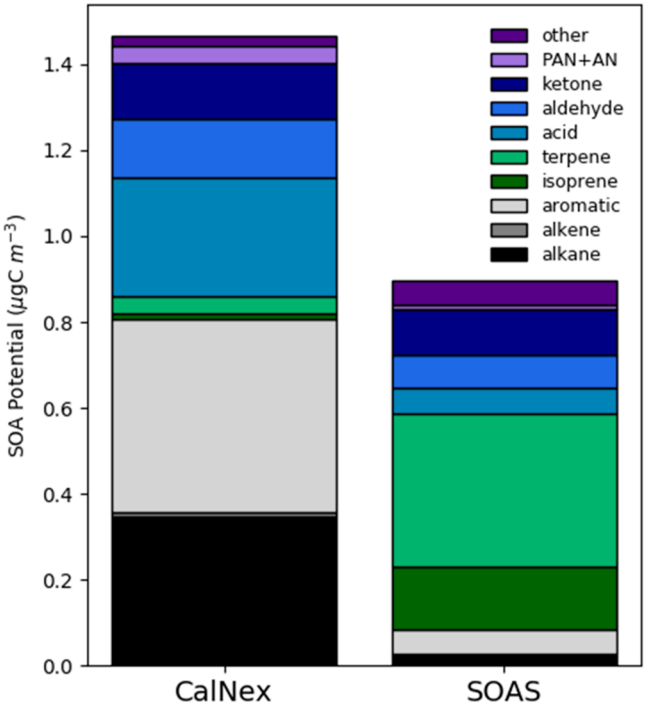

Figure 4. Average estimated SOA potential for CalNex and SOAS field campaigns.

xylenes have the highest SOA potential. Applying the SOA yields from Zhao et al.[33] (see their Tables S5 and S7) to the reported average mass concentrations and assuming an OM:OC of 2 for the SOA formed would give an additional 0.80 μgCsm^{-3} from IVOC. This is equivalent to more than half of the SOA formation potential of all the online measured species, consistent with the major role that IVOCs play in SOA formation in southern California, as suggested by Hayes et al.[54]

The SOA formation potential at SOAS (0.90 μgCsm^{-3}) is a little more than half of that during CalNex. More than half of this is from isoprene and monoterpenes (0.15 and 0.36 μgCsm^{-3}). The dominance of monoterpene SOA is consistent with the analysis of observed SOA concentrations in the SEUS by Zhang et al.[55] This is considerably less than the SOA formation potential of 1.4 μgCsm^{-3} reported for a ponderosa forest site,[15] however, approximately half of the SOA formation potential assessed at that site was estimated to come from previously unmeasured S/IVOCs, some of which are not measured during SOAS. Sesquiterpenes, with their high SOA yields,[56] could also contribute to SOA in this region, however, as noted in Section 3.2, concentrations of these species are small during SOAS and even assuming 100% yield would contribute less than 0.1 μgCsm^{-3} to the SOA potential. Using an apportionment analysis of FIGAERO-CIMS, Lee et al.[57] also rule out any substantial contribution of sesquiterpene SOA to OA measured during SOAS.

SOA formation potential cannot be directly compared to the observed OA concentrations which reflect contributions from up-wind (both primary and secondary), as well as multiphase chemistry. However, for context, we note that observed OA concentrations from CalNex (3.37 μgCsm^{-3}) and SOAS (1.84 μgCsm^{-3}) are both more than double the instantaneous SOA formation potential estimated at these sites. Furthermore, oxidation flow reactor (OFR) measurements during CalNex report an average of 10.5 μgsm^{-3} (~5.25 μgCsm^{-3}),[58] ~1.9 μgCsm^{-3} above ambient loading. Our estimated SOA potential (including IVOCs) of 2.3 μgCsm^{-3}, is similar, but the OFR constraint may suggest that our yields for SOA potential are overestimated. Similar analysis of the SOAS OFR measurements suggest an enhancement over ambient of 1.2 μgCsm^{-3}, ~30% higher than our estimated SOA potential. Thus, the application of estimated yields based primarily on vapor pressures (with the exception of aromatics and primary biogenics, for which we follow Hunter et al.[15]) may overestimate SOA potential in an urban environment and underestimate SOA potential in a biogenic environment. Further exploration of how estimated SOA potential compares with OFR measurements at various sites, particularly with online measurements of S/IVOCs, may provide constraints on assumed SOA yields.

4. DISCUSSION

Reactive organic carbon (ROC) is a key fuel for atmospheric chemical transformations and the production of secondary pollutants. In this study, we contrast the mass concentrations, OH reactivity, and SOA formation potential of ROC in two very different environments in the United States: Southern California and the SEUS. This comparison allows us to explore how these simple metrics can be used to characterize and contrast the local atmospheric environment. We find that the average ROC mass concentration during CalNex is twice that observed during SOAS, with the former dominated by anthropogenic species, and the later characterized by biogenics. Despite these considerable differences, we find that the OHR is similar at the two sites, however, only about half of the cOHR observed during CalNex comes from organics. Thus, the ROC measured in Southern California is, on average, about a factor of 4 less reactive with OH than that in the SEUS. This could translate to much higher ozone production in the SEUS, however NO_x-limitation and lower OH concentrations depress ozone production rates compared to Southern California. In addition, the lower OH in the SEUS extends the isoprene lifetime, increasing the observed reactivity.[59] Finally, the SOA formation potential for all the ROC species measured in CalNex is almost twice that estimated for SOAS, largely driven by aromatics. Thus, we conclude that the ROC species in Southern California are more abundant, less reactive, and (due to the presence of elevated NO_x and OH) more efficiently produce ozone and SOA than the ROC species present in the SEUS.

This analysis is based on a bottom-up characterization of ROC, by adding up the contributions of measured individual species. Given the absence of any top-down total carbon measurement, we cannot assess the degree of mass closure obtained with this suite of measurements. However, the total OHR measurements from these campaigns suggest that the bottom-up tally of cOHR is short by 14% (SOAS) and 31% (CalNex). This missing OHR likely represents some combination of missing primary species and unmeasured secondary products. We highlight throughout the potential role of intermediate volatility species, using as an example the offline measurements made during CalNex.[33] While these species likely make a modest contribution to mass concentrations, OHR, and ozone formation, they may well contribute more than a quarter of the SOA formation potential in that region. This illustrates the importance of characterizing the role of IVOC species in PM formation, particularly in urban environments. For SOAS, the missing reactivity is limited to

https://dx.doi.org/10.1021/acs.est.0c05027
Environ. Sci. Technol. 2020, 54, 14923−14935

the nighttime and is much more modest, perhaps within the uncertainty of the measurements. This raises the interesting question of how measurement and reaction rate uncertainties may dictate the limit of how OHR measurements can be used to constrain ROC.

Of the 112 different organic species measured during CalNex and SOAS, many are not routinely reported in field campaigns or simulated in models, however the importance of these constituents varies with location. For example, the chemical mechanism used in the GEOS-Chem global model represents the majority of the species reported during SOAS, and could represent (individually or lumped) 87−95% of the mass, OHR, and SOA formation potential reported here. This same chemical mechanism could represent 85% of the mass concentrations measured during CalNex, but only 80% of the SOA formation potential and 76% of the OHR. Thus, the more diverse suite of anthropogenic compounds emitted in urban environments may be challenging to represent in current models. The number of species routinely detected by new instrumentation deployed in the field continues to grow (e.g., ref 60), and as future campaigns likely report a greater fraction of the ROC in the atmosphere, it may become more challenging for simplified models to represent this diversity and the resulting chemistry.

The results presented here represent a snapshot in time: 2010 in Southern California, and 2013 in the SEUS. Anthropogenic emissions of many key pollutants and precursors continue to decline in the United States, driven by the Clean Air Act. Thus, the emissions of ROC, as well as the chemical environment into which these species are emitted, are dynamic. In particular, NO_x concentrations in Southern California have decreased considerably since the CalNex campaign. The NO_2 measurements reported at Pasadena (EPA AQS site 06−037−2005) fell by 30% from 2010 to 2019. This alone would imply a decrease in OHR of 7% (1.4 s^{-1}) from 2010. Warneke et al.[21] show that anthropogenic hydrocarbon concentrations in Los Angeles declined at a rate of 7.5%yr^{-1} from 1960 to 2010; it is unclear if that trend has continued over the past decade. Although the ratio of NO_x reactivity to ROC reactivity shown here suggests that Pasadena was, on average, in the VOC-limited regime during CalNex, Griffith et al.[41] suggest that the region was on the cusp of the transition between NO_x-limited and VOC-limited at that time. If indeed NO_x reductions have outpaced decreases in ROC reactivity, then Pasadena could have moved into an NO_x-limited ozone production regime in recent years. Laughner and Cohen[61] suggest that this is the case for the greater Los Angeles region based on trends in satellite-derived NO_x lifetimes. Furthermore, the precipitous decline in OHR in the region suggests that OHR in Southern California is currently substantially lower than OHR in the SEUS, a conclusion which emphasizes the importance of biogenic emissions in driving atmospheric reactivity. This is also illustrative of the potential for the modern urban environment in the United States and elsewhere, to move toward the air quality trajectory of cleaner remote regions.

As shown here, comprehensive ROC measurements alongside ancillary gas-phase measurements and top-down constraints such as OHR can be used to better understand the atmospheric chemical environment and how precursors translate to pollutants of interest. The routine deployment of such measurements is critically needed to accurately characterize the effectiveness of air pollution policies over time.

■ ASSOCIATED CONTENT

Supporting Information

The Supporting Information is available free of charge at https://pubs.acs.org/doi/10.1021/acs.est.0c05027.

Table S1 with reaction rates, SOA yields and ROC mass concentrations, cOHR, and SOA potential for each species measured during SOAS and CalNex (PDF)

■ AUTHOR INFORMATION

Corresponding Author

Colette L. Heald − *Department of Civil and Environmental Engineering, Massachusetts Institute of Technology, Cambridge, Massachusetts 02139, United States;* orcid.org/0000-0003-2894-5738; Email: heald@mit.edu

Authors

Joost de Gouw − *Department of Chemistry and Cooperative Institute for Research in Environmental Sciences, University of Colorado, Boulder, Colorado 80309, United States;* orcid.org/0000-0002-0385-1826

Allen H. Goldstein − *Department of Environmental Science, Policy, and Management and Department of Civil and Environmental Engineering, University of California, Berkeley, California 94720, United States;* orcid.org/0000-0003-4014-4896

Alex B. Guenther − *Department of Earth System Science, University of California, Irvine, California 92697, United States*

Patrick L. Hayes − *Department of Chemistry, University of Colorado, Boulder, Colorado 80309, United States*

Weiwei Hu − *Department of Chemistry and Cooperative Institute for Research in Environmental Sciences, University of Colorado, Boulder, Colorado 80309, United States*

Gabriel Isaacman-VanWertz − *Department of Environmental Science, Policy, and Management, University of California, Berkeley, California 94720, United States;* orcid.org/0000-0002-3717-4798

Jose L. Jimenez − *Department of Chemistry and Cooperative Institute for Research in Environmental Sciences, University of Colorado, Boulder, Colorado 80309, United States;* orcid.org/0000-0001-6203-1847

Frank N. Keutsch − *Department of Chemistry and Chemical Biology, Harvard University, Cambridge, Massachusetts 02138, United States*

Abigail R. Koss − *Cooperative Institute for Research in Environmental Sciences, University of Colorado, Boulder, Colorado 80309, United States; Chemical Sciences Laboratory, National Oceanic and Atmospheric Administration, Boulder, Colorado 80305, United States*

Pawel K. Misztal − *Department of Environmental Science, Policy, and Management, University of California, Berkeley, California 94720, United States;* orcid.org/0000-0003-1060-1750

Bernhard Rappenglück − *Department of Earth and Atmospheric Sciences, University of Houston, Houston, Texas 77204, United States*

James M. Roberts − *Chemical Sciences Laboratory, National Oceanic and Atmospheric Administration, Boulder, Colorado 80305, United States*

Philip S. Stevens − *O'Neill School of Public and Environmental Affairs and Department of Chemistry,*

https://dx.doi.org/10.1021/acs.est.0c05027
Environ. Sci. Technol. 2020, 54, 14923−14935

Indiana University, Bloomington, Indiana 47405, United States; orcid.org/0000-0001-9899-4215

Rebecca A. Washenfelder − *Chemical Sciences Laboratory, National Oceanic and Atmospheric Administration, Boulder, Colorado 80305, United States*

Carsten Warneke − *Cooperative Institute for Research in Environmental Sciences, University of Colorado, Boulder, Colorado 80309, United States; Chemical Sciences Laboratory, National Oceanic and Atmospheric Administration, Boulder, Colorado 80305, United States*

Cora J. Young − *Cooperative Institute for Research in Environmental Sciences, University of Colorado, Boulder, Colorado 80309, United States;* orcid.org/0000-0002-6908-5829

Complete contact information is available at: https://pubs.acs.org/10.1021/acs.est.0c05027

Author Contributions

C.L.H. designed the study and undertook the analysis. J.d.G., G.I.-V.W., A.H.G., A.B.G., P.L.H., W.H., J.L.J., F.N.K., A.R.K. P.K.M., B.R., J.M.R., P.S.S., R.A.W., C.W., and C.J.Y. provided measurements used in the analysis. C.L.H. wrote the paper with input from the coauthors. All authors have given approval to the final version of the manuscript.

Funding

This study was supported by the National Science Foundation (AGS 1936642).

Notes

The authors declare no competing financial interest.

■ ACKNOWLEDGMENTS

We thank the following for measurements used in this work: SOAS: Ron Cohen, Paul Wennberg, John Crounse, Jason St. Clair, Tran Nguyen, Bill Brune, and Dave Worton, as well as from the SEARCH network; CalNex: Barry Lefer, Patrick Veres, and John Holloway during CalNex. We thank Jesse Kroll for useful conversations.

■ REFERENCES

(1) Safieddine, S. A.; Heald, C. L.; Henderson, B. H. The global nonmethane reactive organic carbon budget: A modeling perspective. *Geophys. Res. Lett.* **2017**, *44* (8), 3897−3906.

(2) Guenther, A. B.; Jiang, X.; Heald, C. L.; Sakulyanontvittaya, T.; Duhl, T.; Emmons, L. K.; Wang, X. The Model of Emissions of Gases and Aerosols from Nature version 2.1 (MEGAN 2.1): an extended and updated framework for modeling biogenic emissions. *Geosci. Model Dev.* **2012**, *5*, 1471−1492.

(3) Akagi, S. K.; Yokelson, R. J.; Wiedinmyer, C.; Alvarado, M. J.; Reid, J. S.; Karl, T.; Crounse, J. D.; Wennberg, P. O. Emission factors for open and domestic biomass burning for use in atmospheric models. *Atmos. Chem. Phys.* **2011**, *11* (9), 4039−4072.

(4) Schultz, M. G. *REanalysis of the TROpospheric Chemical Composition over the Past 40 Years*; Max Planck Institute for Meteorology: Julich/Hamburg, Germany, 2007.

(5) Heald, C. L.; Kroll, J. H. The fuel of atmospheric chemistry: Toward a complete description of reactive organic carbon. *Science Advances* **2020**, *6* (6), No. eaay8967.

(6) Heald, C. L.; Ridley, D. A.; Kroll, J. H.; Barrett, S. R. H.; Cady-Pereira, K. E.; Alvarado, M. J.; Holmes, C. D. Contrasting the direct radiative effect and direct radiative forcing of aerosols. *Atmos. Chem. Phys.* **2014**, *14* (11), 5513−5527.

(7) Butler, T.; Lupascu, A.; Coates, J.; Zhu, S. TOAST 1.0: Tropospheric Ozone Attribution of Sources with Tagging for CESM 1.2.2. *Geosci. Model Dev.* **2018**, *11* (7), 2825−2840.

(8) Burnett, R.; Chen, H.; Szyszkowicz, M.; Fann, N.; Hubbell, B.; Pope, C. A.; Apte, J. S.; Brauer, M.; Cohen, A.; Weichenthal, S.; et al. Global estimates of mortality associated with long-term exposure to outdoor fine particulate matter. *Proc. Natl. Acad. Sci. U. S. A.* **2018**, *115* (38), 9592−9597.

(9) IPCC Climate Change 2013: The Physical Science Basis. *Contribution of Working Group I to the Fifth Assessment Report of the Intergovernmental Panel on Climate Change*; Cambridge, Cambridge, U.K., 2013; p 1535.

(10) Goldstein, A. H.; Galbally, I. E. Known and unexplored organic constituents in the earth's atmosphere. *Environ. Sci. Technol.* **2007**, *41* (5), 1514−1521.

(11) Roberts, J. M.; Bertman, S. B.; Jobson, T.; Niki, H.; Tanner, R. Measurement of total nonmethane organic carbon (C-y): Development and application at Chebogue Point, Nova Scotia, during the 1993 North Atlantic Regional Experiment campaign. *J. Geophys. Res.-Atmos.* **1998**, *103* (D11), 13581−13592.

(12) Maris, C.; Chung, M. Y.; Lueb, R.; Krischke, U.; Meller, R.; Fox, M. J.; Paulson, S. E. Development of instrumentation for simultaneous analysis of total non-methane organic carbon and volatile organic compounds in ambient air. *Atmos. Environ.* **2003**, *37*, 149−158.

(13) Yang, M. X.; Fleming, Z. L. Estimation of atmospheric total organic carbon (TOC) - paving the path towards carbon budget closure. *Atmos. Chem. Phys.* **2019**, *19* (1), 459−471.

(14) Heald, C. L.; Goldstein, A. H.; Allan, J. D.; Aiken, A. C.; Apel, E.; Atlas, E. L.; Baker, A. K.; Bates, T. S.; Beyersdorf, A. J.; Blake, D. R.; Campos, T.; Coe, H.; Crounse, J. D.; DeCarlo, P. F.; de Gouw, J. A.; Dunlea, E. J.; Flocke, F. M.; Fried, A.; Goldan, P.; Griffin, R. J.; Herndon, S. C.; Holloway, J. S.; Holzinger, R.; Jimenez, J. L.; Junkermann, W.; Kuster, W. C.; Lewis, A. C.; Meinardi, S.; Millet, D. B.; Onasch, T.; Polidori, A.; Quinn, P. K.; Riemer, D. D.; Roberts, J. M.; Salcedo, D.; Sive, B.; Swanson, A. L.; Talbot, R.; Warneke, C.; Weber, R. J.; Weibring, P.; Wennberg, P. O.; Worsnop, D. R.; Wittig, A. E.; Zhang, R.; Zheng, J.; Zheng, W. Total observed organic carbon (TOOC) in the atmosphere: a synthesis of North American observations. *Atmos. Chem. Phys.* **2008**, *8* (7), 2007−2025.

(15) Hunter, J. F.; Day, D. A.; Palm, B. B.; Yatavelli, R. L. N.; Chan, A. H.; Kaser, L.; Cappellin, L.; Hayes, P. L.; Cross, E. S.; Carrasquillo, A. J.; et al. Comprehensive characterization of atmospheric organic carbon at a forested site. *Nat. Geosci.* **2017**, *10* (10), 748−753.

(16) Yang, Y. D.; Shao, M.; Wang, X. M.; Nolscher, A. C.; Kessel, S.; Guenther, A.; Williams, J. Towards a quantitative understanding of total OH reactivity: A review. *Atmos. Environ.* **2016**, *134*, 147−161.

(17) Mao, J.; Ren, X.; Brune, W. H.; Olson, J. R.; Crawford, J. H.; Fried, A.; Huey, L. G.; Cohen, R. C.; Heikes, B.; Singh, H. B.; Blake, D. R.; Sachse, G. W.; Diskin, G. S.; Hall, S. R.; Shetter, R. E. Airborne measurement of OH reactivity during INTEX-B. *Atmos. Chem. Phys.* **2009**, *9* (1), 163−173.

(18) Dolgorouky, C.; Gros, V.; Sarda-Esteve, R.; Sinha, V.; Williams, J.; Marchand, N.; Sauvage, S.; Poulain, L.; Sciare, J.; Bonsang, B. Total OH reactivity measurements in Paris during the 2010 MEGAPOLI winter campaign. *Atmos. Chem. Phys.* **2012**, *12* (20), 9593−9612.

(19) Travis, K. R.; Heald, C. L.; Allen, H. M.; Apel, E. C.; Arnold, S. R.; Blake, D. R.; Brune, W. H.; Chen, X.; Commane, R.; Crounse, J. D.; Daube, B. C.; Diskin, G. S.; Elkins, J. W.; Evans, M. J.; Hall, S. R.; Hintsa, E. J.; Hornbrook, R. S.; Kasibhatla, P. S.; Kim, M. J.; Luo, G.; McKain, K.; Millet, D. B.; Moore, F. L.; Peischl, J.; Ryerson, T. B.; Sherwen, T.; Thames, A. B.; Ullmann, K.; Wang, X.; Wennberg, P. O.; Wolfe, G. M.; Yu, F. Constraining remote oxidation capacity with ATom observations. *Atmos. Chem. Phys.* **2020**, *20* (13), 7753−7781.

(20) Ryerson, T. B.; Andrews, A. E.; Angevine, W. M.; Bates, T. S.; Brock, C. A.; Cairns, B.; Cohen, R. C.; Cooper, O. R.; de Gouw, J. A.; Fehsenfeld, F. C.; Ferrare, R. A.; Fischer, M. L.; Flagan, R. C.; Goldstein, A. H.; Hair, J. W.; Hardesty, R. M.; Hostetler, C. A.; Jimenez, J. L.; Langford, A. O.; McCauley, E.; McKeen, S. A.; Molina, L. T.; Nenes, A.; Oltmans, S. J.; Parrish, D. D.; Pederson, J. R.; Pierce, R. B.; Prather, K.; Quinn, P. K.; Seinfeld, J. H.; Senff, C. J.; Sorooshian, A.; Stutz, J.; Surratt, J. D.; Trainer, M.; Volkamer, R.;

Williams, E. J.; Wofsy, S. C. The 2010 California Research at the Nexus of Air Quality and Climate Change (CalNex) field study. *Journal of Geophysical Research-Atmospheres* **2013**, *118* (11), 5830−5866.

(21) Warneke, C.; de Gouw, J. A.; Holloway, J. S.; Peischl, J.; Ryerson, T. B.; Atlas, E.; Blake, D.; Trainer, M.; Parrish, D. D. Multiyear trends in volatile organic compounds in Los Angeles, California: Five decades of decreasing emissions. *J. Geophys. Res.-Atmos.* **2012**, *117*, 10.

(22) McDonald, B. C.; de Gouw, J. A.; Gilman, J. B.; Jathar, S. H.; Akherati, A.; Cappa, C. D.; Jimenez, J. L.; Lee-Taylor, J.; Hayes, P. L.; McKeen, S. A.; Cui, Y. Y.; Kim, S. W.; Gentner, D. R.; Isaacman-VanWertz, G.; Goldstein, A. H.; Harley, R. A.; Frost, G. J.; Roberts, J. M.; Ryerson, T. B.; Trainer, M. Volatile chemical products emerging as largest petrochemical source of urban organic emissions. *Science* **2018**, *359* (6377), 760−764.

(23) Isaacman-VanWertz, G.; Sueper, D. T.; Aikin, K. C.; Lerner, B. M.; Gilman, J. B.; de Gouw, J. A.; Worsnop, D. R.; Goldstein, A. H. Automated single-ion peak fitting as an efficient approach for analyzing complex chromatographic data. *J. Chromatogr. A* **2017**, *1529*, 81−92.

(24) Hayes, P. L.; Ortega, A. M.; Cubison, M. J.; Froyd, K. D.; Zhao, Y.; Cliff, S. S.; Hu, W. W.; Toohey, D. W.; Flynn, J. H.; Lefer, B. L.; Grossberg, N.; Alvarez, S.; Rappenglück, B.; Taylor, J. W.; Allan, J. D.; Holloway, J. S.; Gilman, J. B.; Kuster, W. C.; De Gouw, J. A.; Massoli, P.; Zhang, X.; Liu, J.; Weber, R. J.; Corrigan, A. L.; Russell, L. M.; Isaacman, G.; Worton, D. R.; Kreisberg, N. M.; Goldstein, A. H.; Thalman, R.; Waxman, E. M.; Volkamer, R.; Lin, Y. H.; Surratt, J. D.; Kleindienst, T. E.; Offenberg, J. H.; Dusanter, S.; Griffith, S.; Stevens, P. S.; Brioude, J.; Angevine, W. M.; Jimenez, J. L. Organic aerosol composition and sources in Pasadena, California, during the 2010 CalNex campaign. *J. Geophys. Res.-Atmos.* **2013**, *118* (16), 9233−9257.

(25) Worton, D. R.; Kreisberg, N. M.; Isaacman, G.; Teng, A. P.; McNeish, C.; Gorecki, T.; Hering, S. V.; Goldstein, A. H. Thermal Desorption Comprehensive Two-Dimensional Gas Chromatography: An Improved Instrument for In-Situ Speciated Measurements of Organic Aerosols. *Aerosol Sci. Technol.* **2012**, *46* (4), 380−393.

(26) Carlton, A. G.; de Gouw, J.; Jimenez, J. L.; Ambrose, J. L.; Attwood, A. R.; Brown, S.; Baker, K. R.; Brock, C.; Cohen, R. C.; Edgerton, S.; Farkas, C. M.; Farmer, D.; Goldstein, A. H.; Gratz, L.; Guenther, A.; Hunt, S.; Jaegle, L.; Jaffe, D. A.; Mak, J.; McClure, C.; Nenes, A.; Nguyen, T. K.; Pierce, J. R.; de Sa, S.; Selin, N. E.; Shah, V.; Shaw, S.; Shepson, P. B.; Song, S. J.; Stutz, J.; Surratt, J. D.; Turpin, B. J.; Warneke, C.; Washenfelder, R. A.; Wennberg, P. O.; Zhou, X. L. Synthesis of the Southeast Atmosphere Studies: Investigating Fundamental Atmospheric Chemistry Questions. *Bull. Am. Meteorol. Soc.* **2018**, *99* (3), 547−567.

(27) Blanchard, C. L.; Hidy, G. M.; Tanenbaum, S.; Edgerton, E. S.; Hartsell, B. E. The Southeastern Aerosol Research and Characterization (SEARCH) study: Temporal trends in gas and PM concentrations and composition, 1999−2010. *J. Air Waste Manage. Assoc.* **2013**, *63* (3), 247−259.

(28) Ridley, D. A.; Heald, C. L.; Ridley, K. J.; Kroll, J. H. Causes and consequences of decreasing atmospheric organic aerosol in the United States. *Proc. Natl. Acad. Sci. U. S. A.* **2018**, *115* (2), 290−295.

(29) de Gouw, J. A.; Gilman, J. B.; Borbon, A.; Warneke, C.; Kuster, W. C.; Goldan, P. D.; Holloway, J. S.; Peischl, J.; Ryerson, T. B.; Parrish, D. D.; et al. Increasing atmospheric burden of ethanol in the United States. *Geophys. Res. Lett.* **2012**, *39*, 6.

(30) Isaacman-VanWertz, G.; Yee, L. D.; Kreisberg, N. M.; Wernis, R.; Moss, J. A.; Hering, S. V.; de Sa, S. S.; Martin, S. T.; Alexander, M. L.; Palm, B. B.; et al. Ambient Gas-Particle Partitioning of Tracers for Biogenic Oxidation. *Environ. Sci. Technol.* **2016**, *50* (18), 9952−9962.

(31) Isaacman-VanWertz, G.; Lu, X.; Weiner, E.; Smiley, E.; Widdowson, M. Characterization of Hydrocarbon Groups in Complex Mixtures Using Gas Chromatography with Unit-Mass Resolution Electron Ionization Mass Spectrometry. *Anal. Chem.* **2020**, *92* (18), 12481−12488.

(32) Ma, P. K.; Zhao, Y. L.; Robinson, A. L.; Worton, D. R.; Goldstein, A. H.; Ortega, A. M.; Jimenez, J. L.; Zotter, P.; Prevot, A. S. H.; Szidat, S.; Hayes, P. L. Evaluating the impact of new observational constraints on P-S/IVOC emissions, multi-generation oxidation, and chamber wall losses on SOA modeling for Los Angeles, CA. *Atmos. Chem. Phys.* **2017**, *17* (15), 9237−9259.

(33) Zhao, Y. L.; Hennigan, C. J.; May, A. A.; Tkacik, D. S.; de Gouw, J. A.; Gilman, J. B.; Kuster, W. C.; Borbon, A.; Robinson, A. L. Intermediate-Volatility Organic Compounds: A Large Source of Secondary Organic Aerosol. *Environ. Sci. Technol.* **2014**, *48* (23), 13743−13750.

(34) Burkholder, J. B.; Sander, S. P.; Abbatt, J. P.; Barker, J. R.; Huie, R. E.; Kolb, C. E.; Kurylo, M. J.; Orkin, V. L.; Wilmouth, D. M.; Wine, P. H. *Chemical Kinetics and Photochemical Data for Use in Atmospheric Studies, Evaluation No. 18*; Jet Propulsion Laboratory: 2015.

(35) Atkinson, R.; Baulch, D. L.; Cox, R. A.; Crowley, J. N.; Hampson, R. F.; Hynes, R. G.; Jenkin, M. E.; Rossi, M. J.; Troe, J. Evaluated kinetic and photochemical data for atmospheric chemistry: Volume II - gas phase reactions of organic species. *Atmos. Chem. Phys.* **2006**, *6*, 3625−4055.

(36) US EPA *Estimation Programs Interface Suite for Microsoft Windows*, v 4.11.; US EPA: Washington, DC, 2012.

(37) Seinfeld, J. H.; Pandis, S. N. *Atmospheric Chemistry and Physics: From Air Pollution to Climate Change*, 3rd ed.; John Wiley & Sons: New York, 2016; p 1152.

(38) Washenfelder, R. A.; Young, C. J.; Brown, S. S.; Angevine, W. M.; Atlas, E. L.; Blake, D. R.; Bon, D. M.; Cubison, M. J.; de Gouw, J. A.; Dusanter, S.; et al. The glyoxal budget and its contribution to organic aerosol for Los Angeles, California, during CalNex 2010. *J. Geophys. Res.-Atmos.* **2011**, *116* (D21), 17.

(39) de Gouw, J. A.; Gilman, J. B.; Kim, S. W.; Lerner, B. M.; Isaacman-VanWertz, G.; McDonald, B. C.; Warneke, C.; Kuster, W. C.; Lefer, B. L.; Griffith, S. M.; Dusanter, S.; Stevens, P. S.; Stutz, J. Chemistry of Volatile Organic Compounds in the Los Angeles basin: Nighttime Removal of Alkenes and Determination of Emission Ratios. *J. Geophys. Res.-Atmos.* **2017**, *122* (21), 11843−11861.

(40) Feiner, P. A.; Brune, W. H.; Miller, D. O.; Zhang, L.; Cohen, R. C.; Romer, P. S.; Goldstein, A. H.; Keutsch, F. N.; Skog, K. M.; Wennberg, P. O.; Nguyen, T. B.; Teng, A. P.; DeGouw, J.; Koss, A.; Wild, R. J.; Brown, S. S.; Guenther, A.; Edgerton, E.; Baumann, K.; Fry, J. L. Testing Atmospheric Oxidation in an Alabama Forest. *J. Atmos. Sci.* **2016**, *73* (12), 4699−4710.

(41) Griffith, S. M.; Hansen, R. F.; Dusanter, S.; Michoud, V.; Gilman, J. B.; Kuster, W. C.; Veres, P. R.; Graus, M.; Gouw, J. A.; Roberts, J.; et al. Measurements of hydroxyl and hydroperoxy radicals during CalNex-LA: Model comparisons and radical budgets. *J. Geophys. Res.: Atmos.* **2016**, *121* (8), 4211−4232.

(42) Kaiser, J.; Skog, K. M.; Baumann, K.; Bertman, S. B.; Brown, S. B.; Brune, W. H.; Crounse, J. D.; de Gouw, J. A.; Edgerton, E. S.; Feiner, P. A.; et al. Speciation of OH reactivity above the canopy of an isoprene-dominated forest. *Atmos. Chem. Phys.* **2016**, *16* (14), 9349−9359.

(43) Hellen, H.; Praplan, A. P.; Tykka, T.; Ylivinkka, I.; Vakkari, V.; Back, J.; Petaja, T.; Kulmala, M.; Hakola, H. Long-term measurements of volatile organic compounds highlight the importance of sesquiterpenes for the atmospheric chemistry of a boreal forest. *Atmos. Chem. Phys.* **2018**, *18* (19), 13839−13863.

(44) Yee, L. D.; Isaacman-VanWertz, G.; Wernis, R. A.; Meng, M.; Rivera, V.; Kreisberg, N. M.; Hering, S. V.; Bering, M. S.; Glasius, M.; Upshur, M. A.; et al. Observations of sesquiterpenes and their oxidation products in central Amazonia during the wet and dry seasons. *Atmos. Chem. Phys.* **2018**, *18* (14), 10433−10457.

(45) Bouvier-Brown, N. C.; Goldstein, A. H.; Gilman, J. B.; Kuster, W. C.; de Gouw, J. A. In-situ ambient quantification of monoterpenes, sesquiterpenes, and related oxygenated compounds during BEARPEX 2007: implications for gas- and particle-phase chemistry. *Atmos. Chem. Phys.* **2009**, *9* (15), 5505−5518.

(46) Jacob, D. J. *Introduction to Atmospheric Chemistry*; Princeton University Press: Princeton, NJ, 1999.

https://dx.doi.org/10.1021/acs.est.0c05027
Environ. Sci. Technol. 2020, 54, 14923−14935

(47) Sinha, V.; Williams, J.; Diesch, J. M.; Drewnick, F.; Martinez, M.; Harder, H.; Regelin, E.; Kubistin, D.; Bozem, H.; Hosaynali-Beygi, Z.; Fischer, H.; Andres-Hernandez, M. D.; Kartal, D.; Adame, J. A.; Lelieveld, J. Constraints on instantaneous ozone production rates and regimes during DOMINO derived using in-situ OH reactivity measurements. *Atmos. Chem. Phys.* **2012**, *12* (15), 7269−7283.

(48) Bahreini, R.; Middlebrook, A. M.; de Gouw, J. A.; Warneke, C.; Trainer, M.; Brock, C. A.; Stark, H.; Brown, S. S.; Dube, W. P.; Gilman, J. B.; Hall, K.; et al. Gasoline emissions dominate over diesel in formation of secondary organic aerosol mass. *Geophys. Res. Lett.* **2012**, *39* (6), 6.

(49) Silva, S. J.; Heald, C. L. Investigating Dry Deposition of Ozone to Vegetation. *J. Geophys. Res.-Atmos.* **2018**, *123* (1), 559−573.

(50) Kirchner, F.; Jeanneret, F.; Clappier, A.; Kruger, B.; van den Bergh, H.; Calpini, B. Total VOC reactivity in the planetary boundary layer 2. A new indicator for determining the sensitivity of the ozone production to VOC and NOx. *J. Geophys. Res.-Atmos.* **2001**, *106* (D3), 3095−3110.

(51) Matsumoto, J. Measuring Biogenic Volatile Organic Compounds (BVOCs) from Vegetation in Terms of Ozone Reactivity. *Aerosol Air Qual. Res.* **2014**, *14* (1), 197−206.

(52) Jimenez, J. L.; Canagaratna, M. R.; Donahue, N. M.; Prevot, A. S. H.; Zhang, Q.; Kroll, J. H.; DeCarlo, P. F.; Allan, J. D.; Coe, H.; Ng, N. L.; Aiken, A. C.; Docherty, K. S.; Ulbrich, I. M.; Grieshop, A. P.; Robinson, A. L.; Duplissy, J.; Smith, J. D.; Wilson, K. R.; Lanz, V. A.; Hueglin, C.; Sun, Y. L.; Tian, J.; Laaksonen, A.; Raatikainen, T.; Rautiainen, J.; Vaattovaara, P.; Ehn, M.; Kulmala, M.; Tomlinson, J. M.; Collins, D. R.; Cubison, M. J.; Dunlea, E. J.; Huffman, J. A.; Onasch, T. B.; Alfarra, M. R.; Williams, P. I.; Bower, K.; Kondo, Y.; Schneider, J.; Drewnick, F.; Borrmann, S.; Weimer, S.; Demerjian, K.; Salcedo, D.; Cottrell, L.; Griffin, R.; Takami, A.; Miyoshi, T.; Hatakeyama, S.; Shimono, A.; Sun, J. Y.; Zhang, Y. M.; Dzepina, K.; Kimmel, J. R.; Sueper, D.; Jayne, J. T.; Herndon, S. C.; Trimborn, A. M.; Williams, L. R.; Wood, E. C.; Middlebrook, A. M.; Kolb, C. E.; Baltensperger, U.; Worsnop, D. R. Evolution of Organic Aerosols in the Atmosphere. *Science* **2009**, *326* (5959), 1525−1529.

(53) Donahue, N. M.; Robinson, A. L.; Pandis, S. N. Atmospheric organic particulate matter: From smoke to secondary organic aerosol. *Atmos. Environ.* **2009**, *43* (1), 94−106.

(54) Hayes, P. L.; Carlton, A. G.; Baker, K. R.; Ahmadov, R.; Washenfelder, R. A.; Alvarez, S.; Rappenglück, B.; Gilman, J. B.; Kuster, W. C.; de Gouw, J. A.; Zotter, P.; Prevot, A. S. H.; Szidat, S.; Kleindienst, T. E.; Offenberg, J. H.; Ma, P. K.; Jimenez, J. L. Modeling the formation and aging of secondary organic aerosols in Los Angeles during CalNex 2010. *Atmos. Chem. Phys.* **2015**, *15* (10), 5773−5801.

(55) Zhang, H. F.; Yee, L. D.; Lee, B. H.; Curtis, M. P.; Worton, D. R.; Isaacman-VanWertz, G.; Offenberg, J. H.; Lewandowski, M.; Kleindienst, T. E.; Beaver, M. R.; Holder, A. L.; Lonneman, W. A.; Docherty, K. S.; Jaoui, M.; Pye, H. O. T.; Hu, W. W.; Day, D. A.; Campuzano-Jost, P.; Jimenez, J. L.; Guo, H. Y.; Weber, R. J.; de Gouw, J.; Koss, A. R.; Edgerton, E. S.; Brune, W.; Mohr, C.; Lopez-Hilfiker, F. D.; Lutz, A.; Kreisberg, N. M.; Spielman, S. R.; Hering, S. V.; Wilson, K. R.; Thornton, J. A.; Goldstein, A. H. Monoterpenes are the largest source of summertime organic aerosol in the southeastern United States. *Proc. Natl. Acad. Sci. U. S. A.* **2018**, *115* (9), 2038−2043.

(56) Lee, A.; Goldstein, A. H.; Kroll, J. H.; Ng, N. L.; Varutbangkul, V.; Flagan, R. C.; Seinfeld, J. H. Gas-phase products and secondary aerosol yields from the photooxidation of 16 different terpenes. *J. Geophys. Res.-Atmos.* **2006** *111* (D17) DOI: 10.1029/2006JD007050.

(57) Lee, B. H.; D'Ambro, E. L.; Lopez-Hilfiker, F. D.; Schobesberger, S.; Mohr, C.; Zawadowicz, M. A.; Liu, J.; Shilling, J. E.; Hu, W.; Palm, B. B.; Jimenez, J. L.; Hao, L.; Virtanen, A.; Zhang, H.; Goldstein, A. H.; Pye, H. O. T.; Thornton, J. A. Resolving Ambient Organic Aerosol Formation and Aging Pathways with Simultaneous Molecular Composition and Volatility Observations. *ACS Earth and Space Chemistry* **2020**, *4* (3), 391−402.

(58) Ortega, A. M.; Hayes, P. L.; Peng, Z.; Palm, B. B.; Hu, W. W.; Day, D. A.; Li, R.; Cubison, M. J.; Brune, W. H.; Graus, M.; Warneke, C.; Gilman, J. B.; Kuster, W. C.; de Gouw, J.; Gutierrez-Montes, C.; Jimenez, J. L. Real-time measurements of secondary organic aerosol formation and aging from ambient air in an oxidation flow reactor in the Los Angeles area. *Atmos. Chem. Phys.* **2016**, *16* (11), 7411−7433.

(59) Gouw, J. A.; Parrish, D. D.; Brown, S. S.; Edwards, P.; Gilman, J. B.; Graus, M.; Hanisco, T. F.; Kaiser, J.; Keutsch, F. N.; Kim, S. W.; et al. Hydrocarbon Removal in Power Plant Plumes Shows Nitrogen Oxide Dependence of Hydroxyl Radicals. *Geophys. Res. Lett.* **2019**, *46* (13), 7752−7760.

(60) Millet, D. B.; Alwe, H. D.; Chen, X.; Deventer, M. J.; Griffis, T. J.; Holzinger, R.; Bertman, S. B.; Rickly, P. S.; Stevens, P. S.; Leonardis, T.; Locoge, N.; Dusanter, S.; Tyndall, G. S.; Alvarez, S. L.; Erickson, M. H.; Flynn, J. H. Bidirectional Ecosystem-Atmosphere Fluxes of Volatile Organic Compounds Across the Mass Spectrum: How Many Matter. *Acs Earth and Space Chemistry* **2018**, *2* (8), 764−777.

(61) Laughner, J. L.; Cohen, R. C. Direct observation of changing NOx lifetime in North American cities. *Science* **2019**, *366* (6466), 723−727.

(62) Rappenglück, B.; Dasgupta, P. K.; Leuchner, M.; Li, Q.; Luke, W. Formaldehyde and its relation to CO, PAN, and SO2 in the Houston-Galveston airshed. *Atmos. Chem. Phys.* **2010**, *10* (5), 2413−2424.

(63) Roberts, J. M.; Marchewka, M.; Bertman, S. B.; Sommariva, R.; Warneke, C.; de Gouw, J.; Kuster, W.; Goldan, P.; Williams, E.; Lerner, B. M.; et al. Measurements of PANs during the New England air quality study 2002. *J. Geophys. Res.* **2007**, *112* (D20), 14.

(64) Veres, P. R.; Roberts, J. M.; Cochran, A. K.; Gilman, J. B.; Kuster, W. C.; Holloway, J. S.; Graus, M.; Flynn, J.; Lefer, B.; Warneke, C.; de Gouw, J. Evidence of rapid production of organic acids in an urban air mass. *Geophys. Res. Lett.* **2011**, *38* (17), 5.

(65) Kuster, W. C.; Jobson, B. T.; Karl, T.; Riemer, D.; Apel, E.; Goldan, P. D.; Fehsenfeld, F. C. Intercomparison of volatile organic carbon measurement techniques and data at la porte during the TexAQS2000 Air Quality Study. *Environ. Sci. Technol.* **2004**, *38* (1), 221−228.

(66) Warneke, C.; Kato, S.; De Gouw, J. A.; Goldan, P. D.; Kuster, W. C.; Shao, M.; Lovejoy, E. R.; Fall, R.; Fehsenfeld, F. C. Online volatile organic compound measurements using a newly developed proton-transfer ion-trap mass spectrometry instrument during New England Air Quality Study - Intercontinental Transport and Chemical Transformation 2004: Performance, intercomparison, and compound identification. *Environ. Sci. Technol.* **2005**, *39* (14), 5390−5397.

(67) Hansen, R. F.; Griffith, S. M.; Dusanter, S.; Rickly, P. S.; Stevens, P. S.; Bertman, S. B.; Carroll, M. A.; Erickson, M. H.; Flynn, J. H.; Grossberg, N.; Jobson, B. T.; Lefer, B. L.; Wallace, H. W. Measurements of total hydroxyl radical reactivity during CABINEX 2009-Part 1: field measurements. *Atmos. Chem. Phys.* **2014**, *14* (6), 2923−2937.

(68) Lefer, B.; Rappenglück, B.; Flynn, J.; Haman, C. Photochemical and meteorological relationships during the Texas-II Radical and Aerosol Measurement Project (TRAMP). *Atmos. Environ.* **2010**, *44* (33), 4005−4013.

(69) Luke, W. T.; Kok, G. L.; Schillawski, R. D.; Zimmerman, P. R.; Greenberg, J. P.; Kadavanich, M. TRACE GAS MEASUREMENTS IN THE KUWAIT OIL FIRE SMOKE PLUME. *J. Geophys. Res.* **1992**, *97* (D13), 14499−14506.

(70) Pollack, I. B.; Lerner, B. M.; Ryerson, T. B. Evaluation of ultraviolet light-emitting diodes for detection of atmospheric NO2 by photolysis - chemiluminescence. *J. Atmos. Chem.* **2010**, *65* (2−3), 111−125.

(71) Drummond, J. W.; Volz, A.; Ehhalt, D. H. AN OPTIMIZED CHEMI-LUMINESCENCE DETECTOR FOR TROPOSPHERIC NO MEASUREMENTS. *J. Atmos. Chem.* **1985**, *2* (3), 287−306.

(72) Gerbig, C.; Schmitgen, S.; Kley, D.; Volz-Thomas, A.; Dewey, K.; Haaks, D. An improved fast-response vacuum-UV resonance fluorescence CO instrument. *J. Geophys. Res.-Atmos.* **1999**, *104* (D1), 1699−1704.

(73) Hu, W. W.; Palm, B. B.; Day, D. A.; Campuzano-Jost, P.; Krechmer, J. E.; Peng, Z.; de Sa, S. S.; Martin, S. T.; Alexander, M. L.; Baumann, K.; Hacker, L.; Kiendler-Scharr, A.; Koss, A. R.; de Gouw, J. A.; Goldstein, A. H.; Seco, R.; Sjostedt, S. J.; Park, J. H.; Guenther, A. B.; Kim, S.; Canonaco, F.; Prevot, A. S. H.; Brune, W. H.; Jimenez, J. L. Volatility and lifetime against OH heterogeneous reaction of ambient isoprene-epoxydiols-derived secondary organic aerosol (IEPOX-SOA). *Atmos. Chem. Phys.* **2016**, *16* (18), 11563−11580.

(74) DiGangi, J. P.; Boyle, E. S.; Karl, T.; Harley, P.; Turnipseed, A.; Kim, S.; Cantrell, C.; Maudlin, R. L.; Zheng, W.; Flocke, F.; Hall, S. R.; Ullmann, K.; Nakashima, Y.; Paul, J. B.; Wolfe, G. M.; Desai, A. R.; Kajii, Y.; Guenther, A.; Keutsch, F. N. First direct measurements of formaldehyde flux via eddy covariance: implications for missing in-canopy formaldehyde sources. *Atmos. Chem. Phys.* **2011**, *11* (20), 10565−10578.

(75) Hottle, J. R.; Huisman, A. J.; Digangi, J. P.; Kammrath, A.; Galloway, M. M.; Coens, K. L.; Keutsch, F. N. A Laser Induced Fluorescence-Based Instrument for In-Situ Measurements of Atmospheric Formaldehyde. *Environ. Sci. Technol.* **2009**, *43* (3), 790−795.

(76) Huisman, A. J.; Hottle, J. R.; Coens, K. L.; DiGangi, J. P.; Galloway, M. M.; Kammrath, A.; Keutsch, F. N. Laser-induced phosphorescence for the in situ detection of glyoxal at part per trillion mixing ratios. *Anal. Chem.* **2008**, *80* (15), 5884−5891.

(77) Nguyen, T. B.; Crounse, J. D.; Teng, A. P.; St Clair, J. M.; Paulot, F.; Wolfe, G. M.; Wennberg, P. O. Rapid deposition of oxidized biogenic compounds to a temperate forest. *Proc. Natl. Acad. Sci. U. S. A.* **2015**, *112* (5), E392−E401.

(78) Romer, P. S.; Duffey, K. C.; Wooldridge, P. J.; Allen, H. M.; Ayres, B. R.; Brown, S. S.; Brune, W. H.; Crounse, J. D.; de Gouw, J.; Draper, D. C.; Feiner, P. A.; Fry, J. L.; Goldstein, A. H.; Koss, A.; Misztal, P. K.; Nguyen, T. B.; Olson, K.; Teng, A. P.; Wennberg, P. O.; Wild, R. J.; Zhang, L.; Cohen, R. C. The lifetime of nitrogen oxides in an isoprene-dominated forest. *Atmos. Chem. Phys.* **2016**, *16* (12), 7623−7637.

(79) Gilman, J. B.; Burkhart, J. F.; Lerner, B. M.; Williams, E. J.; Kuster, W. C.; Goldan, P. D.; Murphy, P. C.; Warneke, C.; Fowler, C.; Montzka, S. A.; Miller, B. R.; Miller, L.; Oltmans, S. J.; Ryerson, T. B.; Cooper, O. R.; Stohl, A.; de Gouw, J. A. Ozone variability and halogen oxidation within the Arctic and sub-Arctic springtime boundary layer. *Atmos. Chem. Phys.* **2010**, *10* (21), 10223−10236.

(80) Graus, M.; Muller, M.; Hansel, A. High Resolution PTR-TOF: Quantification and Formula Confirmation of VOC in Real Time. *J. Am. Soc. Mass Spectrom.* **2010**, *21* (6), 1037−1044.

(81) Faloona, I. C.; Tan, D.; Lesher, R. L.; Hazen, N. L.; Frame, C. L.; Simpas, J. B.; Harder, H.; Martinez, M.; Di Carlo, P.; Ren, X. R.; Brune, W. H. A laser-induced fluorescence instrument for detecting tropospheric OH and HO2: Characteristics and calibration. *J. Atmos. Chem.* **2004**, *47* (2), 139−167.

https://dx.doi.org/10.1021/acs.est.0c05027
Environ. Sci. Technol. 2020, 54, 14923−14935